# Dry spinning yarns from vertically aligned carbon nanotube arrays produced by an improved floating catalyst chemical vapor deposition method

Qiang Zhang *, Dong-Guang Wang, Jia-Qi Huang, Wei-Ping Zhou, Guo-Hua Luo, Wei-Zhong Qian, Fei Wei **

Beijing Key Laboratory of Green Reaction Engineering and Technology, Department of Chemical Engineering, Tsinghua University, Beijing 100084, China

ARTICLE INFO

ABSTRACT

Carbon nanotube (CNT) yarn was drawn directly from super aligned CNT arrays synthesized by an improved floating catalyst chemical vapor deposition method. The synthesis of aligned CNT was performed as a multi-step interim reactant supply reaction to produce a double-layered CNT array in a horizontal quartz tube reactor. During the growth period, most impurities were blocked on the top surface of the first layer and therefore the top aligned CNT layer was unspinnable. However, the bottom CNT layer was super aligned CNTs, which were with clean surface and a tortuosity factor of 1.07. During the dry spinning process, the tangles, friction, and van der Waals interaction between CNTs served to hold them into CNT yarns. The tensile strength of the as-obtained CNT yarn can be further improved from 0.24 to 0.30 GPa by twisting.

## 1. Introduction

Creating carbon nanotubes (CNTs) with macroscopic lengths is necessary to make use of the exceptional physical properties of CNTs at a macroscopic level. Various forms of macroscopic CNTs, such as horizontally aligned CNTs on flat substrates [1], long vertically aligned CNTs [2], CNT strands [3–5], CNT yarns [6–8], and CNT composite fibers [9,10], have been obtained. Among various macroscopic CNTs, CNT yarns simply by being drawn out from super aligned arrays of CNTs attracted great attention for their great mechanical strength, especially after twisting [7,11–13]. CNT yarns also show effective electrical transport, optical transmittance, and light emission properties [6–8]. Further applications, such as filaments for heaters [11], field emission display [14], polarizers working in the ultraviolet region [6], and actuators [15] are re-ported. These applications can become feasible in daily life if the CNT yarn can be produced in large scale and at a low cost.

Macroscopic CNT yarn can be directly spun from a super aligned CNT array obtained by thermal chemical vapor deposition (CVD), which was first demonstrated by Jiang et al. in 2002 [6]. Later, Zhang et al. and Li et al. reported that a multi-functional CNT film/fiber can be obtained from an aligned CNT array [7,8,16,17]. The length of the CNT yarn was arbitrary, and the diameter of the yarn could be easily modulated during the spinning process [6]. However, the reported spinnable CNT arrays were all grown on wafers by thermal CVD. The aligned CNT growth by the thermal CVD method is accomplished in a reaction furnace with flowing gaseous carbon feedstock in the presence of catalyst on a wafer. A catalyst film, such as $Fe/Al_2O_3$, must be deposited on a wafer through a complicated process before

---

the growth of CNT arrays [6–8,16–21]. Developing a facile spinnable super aligned CNT synthesis strategy is still a great challenge.

It should be noticed that another popular method for the synthesis of aligned CNTs is floating catalyst CVD [22–24]. The catalyst precursors, such as metal carbonyls and metallocenes, are fed into the horizontal or vertical reactor together with the carbon source. The catalyst particles for the growth of CNT arrays form *in situ*, and aligned CNTs grow at a temperature ranging from 550 to 850 °C. This method requires simple equipments and eliminates the procedure for the pre-preparation of catalyst layers. Usually, a single layer of aligned CNTs were obtained on a flat [22–25] or a spherical substrate [26]. The previously reported aligned CNT arrays by floating catalyst CVD were usually unspinnable [22–27]. Delicate controls for complicated super aligned CNT synthesis and a general understanding between the aligned CNT array structure and spinnability are still needed.

In this report, spinnable CNT arrays were obtained for the first time through an improved floating catalyst CVD method. The synthesis of aligned CNT array was performed as a multi-step interim reactant supply reaction to produce a double-layered CNT array, in which the top CNT layer was unspinnable, and the second CNT layer was spinnable. The relationship between the CNT array structure and spinnability was shown, which provided a further understanding for the production of CNT yarns.

## 2. Experimental

Spinnable carbon nanotube (CNT) arrays were synthesized by the improved floating catalyst CVD using ferrocene (analytical reagent grade, A.R.) as the catalyst precursor, and cyclohexane (A.R.) as the carbon source. The concentration of ferrocene in the cyclohexane is 10 g/L. A horizontal quartz tube with an inner diameter of 26.5 mm and a length of 1500 mm served as their reactor, as well as the growth substrate. The reactor designs are similar to our previous reports [28]. Before the growth of CNT arrays, the quartz tube was soaked in a hydrofluoric acid solution (2%) for 24 h, rinsed with flowing deionized water, and then dried in air.

For aligned CNT growth, the quartz tube was laid into a two-stage furnace. The first stage of the furnace was used to vaporize the solution at a temperature of ca. 350 °C, and the second stage was used to synthesize aligned CNT arrays at a temperature of 810 °C. Cyclohexane solution, at a feed rate of 5.0 mL/h, was injected by a motorized syringe pump into the reactor at the first stage of the furnace. Meanwhile, a carrier gas of 80% Ar (99.9995%) and 20% $H_2$ (99.9995%) with a flow rate of 800 sccm was also introduced into the reactor. The carbon source was decomposed by the *in situ* formed metal catalyst particles for the growth of aligned CNTs in the second stage for half an hour. Then the feed of cyclohexane solution was stopped and the second stage of the furnace was cooled to 300 °C under the protection of Ar. The second stage was again heated to the growth temperature for the growth of second aligned CNT array layer. The CNTs can therefore be synthesized as arrays in two layers. A multi-lay-

ered aligned CNT synthesis can be obtained through the multi-step interim reactant supply reaction. Most of the contamination from the gaseous impurities was blocked by the first top layer of the array; the aligned CNT arrays under the first layer had a clean top surface. For the final cooling, 100 sccm $CO_2$ was introduced into the reactor to minimize the interaction between the aligned CNTs and the quartz substrate [29].

The CNT array was harvested from the substrate by a razor blade. It was found that CNT yarn could be continuously spun from the aligned CNT synthesized through the improved floating catalyst CVD method. Photos and videos of spinning the CNT yarn from aligned CNTs were taken using a Ricoh R4 video camera. In the post-spin twisting process, a 3 M tape was attached to one end of a CNT yarn to provide tension in the axial direction, while the other end of the fiber was attached to a rotator. A 4-cm-long CNT yarn was typically twisted at a rotation rate of 100 rpm.

The morphology of the product was visualized using a JEOL JSM 7401F scanning electron microscope (SEM) operated at 3.0 kV and a JEOL JEM 2010 transmission electron microscope (TEM) operated at 120.0 kV. Raman experiments were performed using a Renishaw RM2000 Raman spectrophotometer. The purity of the CNTs in the as-grown product was measured using thermal gravimetric analysis by TGA Q500. The tensile strength of the CNT fiber was measured by an YG0001B fiber tester. The CNT fibers were mounted on paper tabs with a gauge length of 15 mm. The fiber diameter was measured from the SEM photograph. The tensile speed was 0.04 mm s$^{-1}$.

## 3. Results and discussion

### 3.1. Dry spin yarns from super aligned CNT arrays produced by an improved floating catalyst CVD method

As shown in the video (Supplementary material) and Fig. 1a, CNT yarn was continuously spun from the second layer of the CNT arrays. There was no limitation on the physical length of the CNT yarn. The spun out CNTs connected with the remaining CNTs in the array end-to-end. Effective, continuous transfer of connections between CNTs is the key factor during the spinning process. Nodes were produced by the interaction of the CNTs. Three kinds of connections among CNTs were found after detailed observation, as shown in Fig. 1b–d.

The first kind of connection is the tangle as shown in Fig. 1b, which was formed by the connection of amorphous carbon, the carbon spheres with the inner catalyst, and the related CNTs (Fig. 2a). They were jointed by chemical bonds between the carbon and the Fe catalyst. The contribution of tangles around the Fe catalyst as connections among CNTs was quite low. It should be noticed that too high density of tangles is negative to the spinnability of aligned CNTs. The second kind of connection was formed by the friction between the twisted CNTs at the end of the CNT arrays (Fig. 1c). There were entanglements among CNTs at the end of the array (Fig. 2b–d). Once the CNT bundles were peeled from the substrate, the entanglements among CNTs
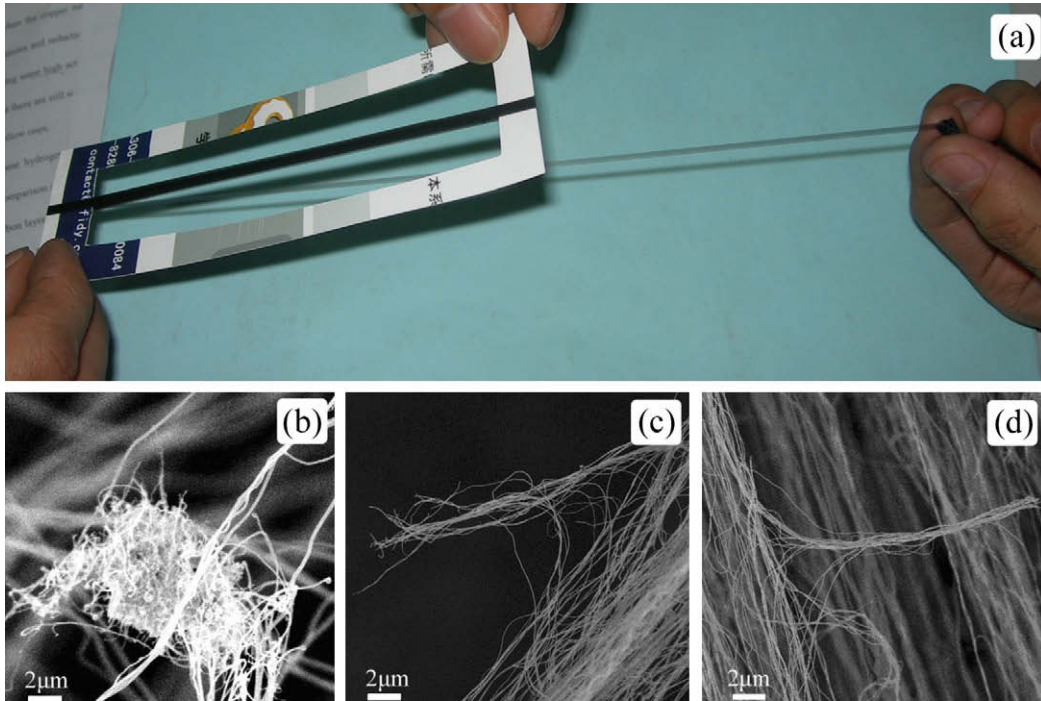
**Fig. 1 – (a) Spun CNT yarn from the CNT array produced by the floating catalyst process. (b–d) Typical connection types of CNTs in the CNT yarn.**
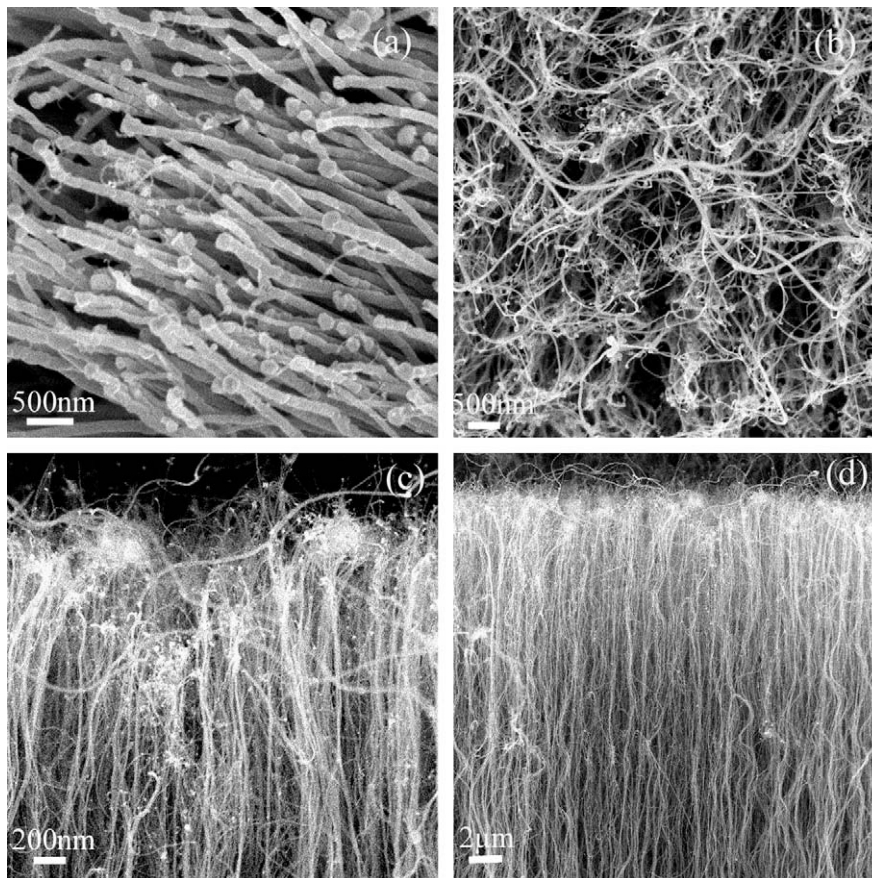


**Fig. 2 – (a) The bottom view of the spinnable CNT array. (b) The top view of the spinnable CNT array. (c and d) Cross-view morphology of the spinnable CNT array.**

induced the friction between CNT bundles. The third interaction is the van der Waals interaction between CNTs (Figs. 1d and S1). The van der Waals attraction is a large contribution to the adhesions among CNTs, which is believed to be the most important interaction for spinnable thin-walled CNT arrays obtained by thermal CVD [6–8,16–19]. The van der Waals adhesion is a close-range force, and is the dominant interaction among small diameter CNTs. In previous reports, spinnable CNT arrays produced by thermal CVD have a diameter less than 10 nm [16–19]. In the present study, the diameter of the CNTs produced by floating catalyst CVD was about 35 nm. The number density of the CNTs in the spinnable array was about $1 \times 10^{13}$ CNT/m$^2$. This is larger than those obtained by a common floating catalyst CVD ($4.6 \times 10^{12}$ CNT/m$^2$). High density CNTs corresponded to more connections of CNT ends, indicating a stronger van der Waals adhesion. During the spinning process, the van der Waals attraction can hold CNTs into yarn for continuous spinning.

## 3.2. The characteristics of super aligned CNT arrays produced by an improved floating catalyst CVD method

Most of CNT arrays obtained by common floating catalyst CVD are unspinnable. The spinnable CNT array obtained in this article exhibits the following characteristics.

Firstly, the second layer of the array was spinnable, while the first layer was unspinnable. During the multi-stage growth procedure, most of the impurities were deposited on the top surface of the first layer [28]. Then the top layer of CNTs was always unspinnable. This is a main reason for that CNTs grown by a common floating catalyst CVD were commonly unspinnable [22,23,25–27,30,31]. Moreover, the top surface of the second layer is very clean. Fewer impurities can be found in spinnable CNT array (second layer), as indicated by Fig. 2.

Secondly, the alignment of CNTs has been greatly improved. As shown in Fig. 3a, both Types 1 (straight) and 2 (curved) CNTs can be found in the spinnable CNT array. The
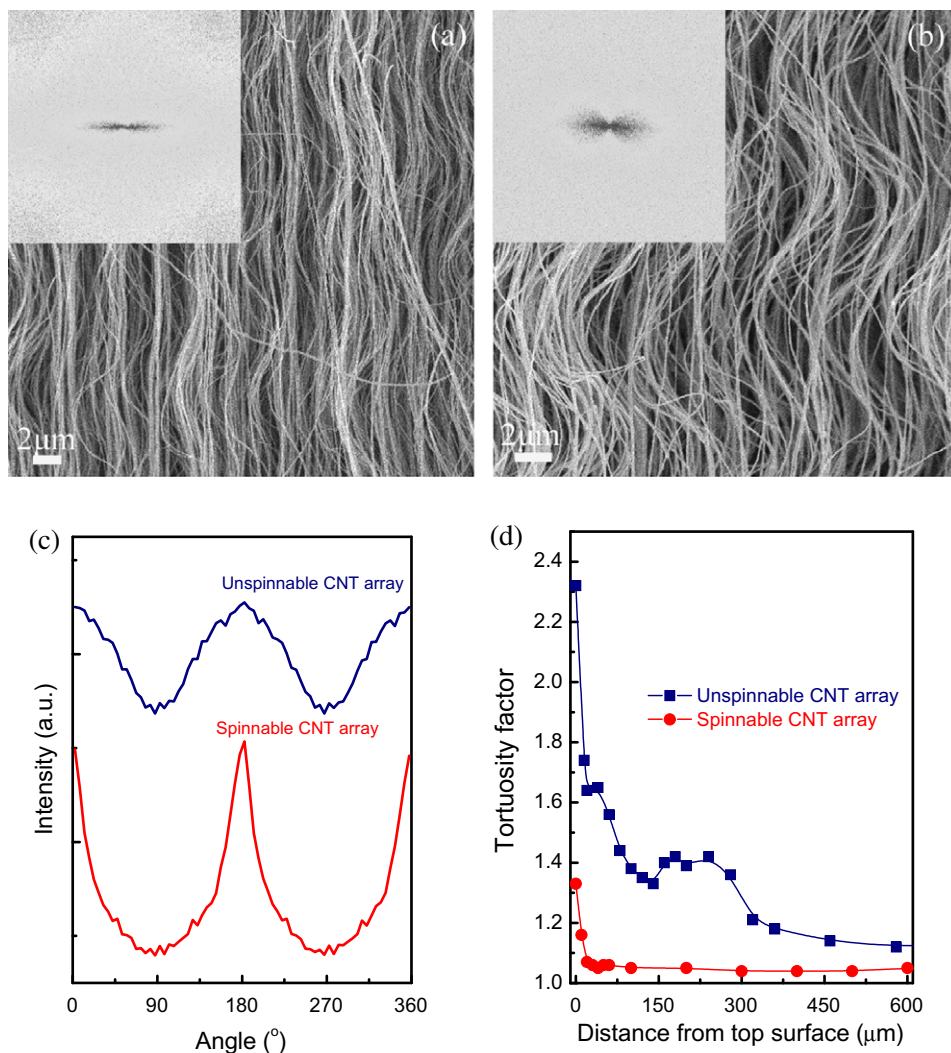


Fig. 3 – The morphology of (a) spinnable and (b) unspinnable CNT arrays. Inserted figures in (a) and (b) are the power spectra of the related SEM images. (c) The angular intensity of the power spectrum. (d) The tortuosity factors of Type 2 CNTs in the array.

**Table 1 – Comparison between unspinnable and spinnable CNT arrays.**

|  | Unspinnable CNT array | Spinnable CNT array-A | Spinnable CNT array-B |
|---|---|---|---|
| CVD methods | Floating catalyst | Floating catalyst | Thermal |
| Growth temperature (°C) | 600–900 | 780–830 | 680–750 |
| Length (μm) | 1–8000 | 200–700 | 150–900 |
| Densities (CNTs/m$^2$) | $\sim 4.6 \times 10^{12}$ | $\sim 1 \times 10^{13}$ | $2.5–10 \times 10^{14}$ |
| Mean diameter (nm) | $\sim 40$ | $\sim 35$ | $\sim 6.6$ |
| Standard deviation of diameter (nm) | $\sim 9$ | $\sim 3$ | 1–2 |
| Transition length (μm) | $\sim 120$ | $\sim 30$ | – |
| Tortuosity factor | $\sim 1.30$ | $\sim 1.07$ | $\sim 1.06$ |
| $I_D/I_G$ | 0.8–1.5 | 0.8 | 0.5 |
| Purity (%) | $\sim 97$ | $\sim 99$ | – |
| Refs. | [28] | This work | [11,14,18] |

power spectrum [32,33], which was obtained by fast Fourier transform (FFT) of related SEM images, was shown in the inserted figure of Fig. 3a. The SEM image and power spectrum of unspinnable CNT array were shown in Fig. 3b. A sharp peak can be found in the angular intensity of the power spectrum for the spinnable CNT array, as indicated by Fig. 3c. The orientation state factor for the spinnable array was estimated to be 0.93, and the tortuosity factor [28] of spinnable CNTs was 1.07 after 30 μm from the top surface (Fig. 3d). For the unspinnable CNT array, the tortuosity factor was obviously higher than 1.30 at the initial 300 μm (Fig. 3d).

The detailed comparisons among the unspinnable array [28], the spinnable array-A obtained by floating catalyst CVD, and the spinnable array-B obtained by thermal CVD [11,18], are shown in Table 1. The spinnable array possesses a large number density and a small tortuosity factor. Super aligned CNTs with good orientation and uniform diameter were required in the spinnable array. The diameter of the spinnable CNTs obtained by floating catalyst CVD was obviously larger than those obtained by thermal CVD. It demonstrated similar mean diameter to that of the unspinnable array, but with a smaller standard deviation. In the improved floating catalyst CVD method, a multi-stage growth was carried out, and catalyst particles with a high density were

deposited on the quartz tube. Compared with unspinnable CNT arrays (such as the first layer), the spinnable CNT arrays are with a higher density and a shorter transition distance (Figs. 2 and 3d), which can be attributed to the space limitation of the first layer during CNT nucleation and uniform catalyst particle formation. Furthermore, the Types 1 and 2 CNTs with small differences in both the growth rate and the diameter distribution were synthesized by a synchronous growth, and thus the super aligned structure was obtained. The $CO_2$ introduction during the cooling process weakened the connection between CNT array and substrate and facilitated the free-standing spinnable CNT harvest [29].

### 3.3. The properties of CNT yarns

Large amount of CNT yarns can be obtained from the super aligned CNTs produced by the improved floating catalyst CVD method. A typical as-obtained CNT yarn was shown in Fig. 4a. The as-spun fiber is relatively loose with noticeable spaces between CNTs or CNT bundles. The tensile strength was approximately 0.24 GPa. To improve the tensile strength of the CNT yarn, post-spin twisting was carried out. The twisted CNT fiber was shown in Fig. 4b. The diameter of the CNT fiber decreased to about 10 μm and its strength increased
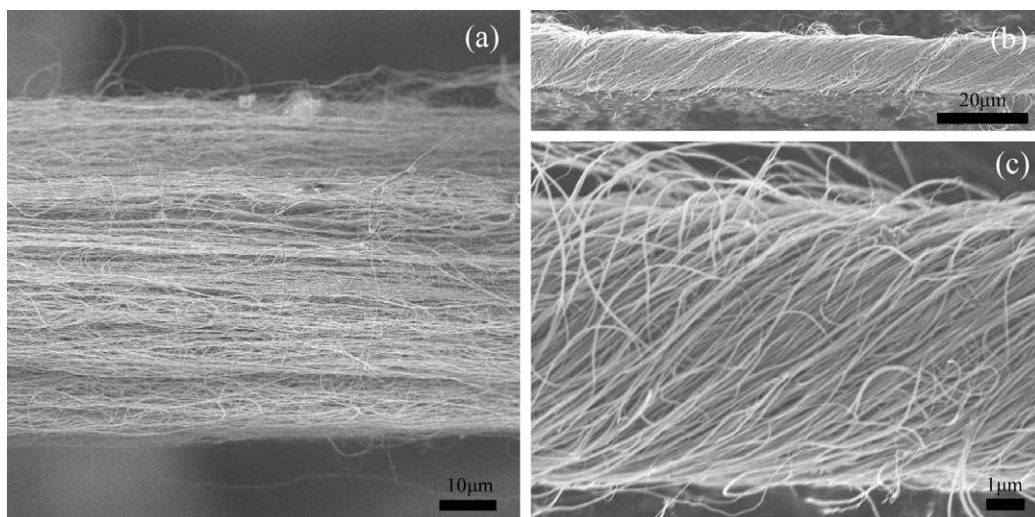


**Fig. 4 – (a) The yarn obtained by directly spinning the CNTs produced by floating catalyst CVD. (b and c) The fiber after post-spin twisting.**

to 0.3 GPa. This was attributed to the fact that the CNTs were in closer contact with each other, thus enhancing the van der Waals adhesion and friction, which improved the load transfer between the CNTs. However, the tensile strength is still smaller than those of twisted CNT yarn obtained from thermal CVD (usually 0.15–1.91 GPa [7,12]). In general, the tensile strength of a twisted fiber can be described by the following equation [7,12]:

$$\frac{\delta_f}{\delta_{CNT}} \approx \cos\alpha \left[ 1 - \left( \frac{(dQ/\mu)^{1/2}/3L}{\sin\alpha} \right) \right] \qquad (1)$$

where $\delta_f$ and $\delta_{CNT}$ are the tensile strengths of the twisted fiber and the CNT, respectively; $\alpha$ is the twist angle, $d$ is the CNT diameter, $L$ is the CNT length, $\mu$ is the friction coefficient between CNTs, and $L$ is the CNT migration length. Here, the diameter of the CNTs in the present study was 30–40 nm, which was obviously larger than that obtained from previous mentioned thermal CVD (3–10 nm) [6–8,16–19]. The $I_D/I_G$ ratio illustrated in Table 1 indicated more defects could be found on super aligned CNTs obtained through floating catalyst CVD compared with those on CNTs obtained through thermal CVD [14,28]. Moreover, the predicted tensile strength of multi-walled CNT ($\delta_{CNT}$) decreased with increasing the diameters of multi-walled CNTs [34]. As indicated by Eq. (1), the fiber strength ($\delta_f$) decreases with increasing the diameter of CNTs. During the twisting process, the alignment of CNTs turn bad, and some of CNTs scattered from the fiber (Fig. 4c). Main parts of CNTs were held together with a surface twisting angel of 40°. If the CNTs can be held closely, the fiber probably breaks due to relative sliding between CNTs attributed from large diameter, and low contact area. As illustrated by Zhang et al. [12], the increase in load capacity by post-spin twisting is caused by stronger inter-CNT interaction and higher radial-compressive stress. The stronger inter-CNT interactions attribute from the closer inter-CNT distance after the twisting, which increases the van der Waals adhesion along individual CNTs. The radial-compressive stress increases with the tensile stress during the fiber-tensile testing, which increases the effectiveness of load transfer via mechanical interlocking between the CNTs [12]. Thus, CNTs with small diameter and long length are easy to form large contact area for strong fiber with an optimized twisting angles and twisting procedure. This consisted well with the tensile strength of a twisted fiber, as illustrated by Eq. (1). Recently, using molecular dynamics simulation, Zhang et al. reported the inter-tube frictional force could be increased by a factor of 1.5–4, depending on tube chirality and radius of single walled CNTs, when all tubes collapse and when the bundle remains collapsed with unloading down to atmospheric pressure [35]. Based on those analyses, growth of small diameter super aligned CNTs by the optimized improved floating catalyst CVD method is still a necessary step to obtain strong CNT fibers.

Finally, it should be noticed that bulk long CNT strands were firstly fabricated by Cheng et al. through floating catalyst CVD 10 years ago [3,4]. The long CNT strands over 20 cm in length with a tensile strength of 0.8–1.1 GPa [5] and continuously spinning of CNT fiber from the reactor [36–38] were also reported. However, the reported CNT strands generated by the floating catalyst process were obtained at a temperature above

1000 °C [3–5,36–38]. The present reported improved method required a lower temperature (800 °C) for the growth of super aligned CNT arrays. Various process intensification strategies for aligned CNTs synthesis, such as chloride mediated catalyst [39], combination between catalyst formation, reduction, and continuous growth [18,21], natural resources for low cost synthesis [40,41], floating substrate for high aspect-ratio CNT "flying carpets" growth [42], has been developed. There is still scope for further exploration of CNT yarns with extraordinary mechanical, thermal and electrical properties obtained by the improved floating catalyst CVD method.

## 4.    Conclusions

A CNT yarn spinning process from super aligned CNT arrays produced by an improved floating catalyst method was reported. The CNTs in the super aligned array had a tortuosity factor of 1.07, and an orientation state factor of 0.93. The tangles, friction, and van der Waals interactions between the CNTs provided connections between the CNTs during the spinning process. Then CNT yarn could be continuously drawn from the arrays. Since there was no pre-deposition of catalyst or high temperature (over 1000 °C) treatment, an easy method to prepare spinnable CNT array was provided, which is of significance for potential applications of CNTs.

## Acknowledgements

## Appendix A.    Supplementary data

A video CNT yarn spinning from an aligned CNT array, and a TEM image are provided and are available online. Supplementary data associated with this article can be found, in the online version, at doi:10.1016/j.carbon.2010.04.017.

REFERENCES

[1] Liu ZF, Jiao LY, Yao YG, Xian XJ, Zhang J. Aligned, ultralong single-walled carbon nanotubes: from synthesis, sorting, to electronic devices. Adv Mater 2010;22. doi:10.1002/adma.20090416.
[2] Li XS, Zhang XF, Ci LJ, Shah R, Wolfe C, Kar S, et al. Air-assisted growth of ultra-long carbon nanotube bundles. Nanotechnology 2008;19(45):455609/1–7.
[3] Cheng HM, Li F, Su G, Pan HY, He LL, Sun X, et al. Large-scale and low-cost synthesis of single-walled carbon nanotubes by the catalytic pyrolysis of hydrocarbons. Appl Phys Lett 1998;72(25):3282–4.

[4] Cheng HM, Li F, Sun X, Brown SDM, Pimenta MA, Marucci A, et al. Bulk morphology and diameter distribution of single-walled carbon nanotubes synthesized by catalytic decomposition of hydrocarbons. Chem Phys Lett 1998;289(5–6):602–10.

[5] Zhu HW, Xu CL, Wu DH, Wei BQ, Vajtai R, Ajayan PM. Direct synthesis of long single-walled carbon nanotube strands. Science 2002;296(5569):884–6.

[6] Jiang KL, Li QQ, Fan SS. Nanotechnology: spinning continuous carbon nanotube yarns – carbon nanotubes weave their way into a range of imaginative macroscopic applications. Nature 2002;419(6909):801.

[7] Zhang M, Atkinson KR, Baughman RH. Multifunctional carbon nanotube yarns by downsizing an ancient technology. Science 2004;306(5700):1358–61.

[8] Zhang M, Fang SL, Zakhidov AA, Lee SB, Aliev AE, Williams CD, et al. Strong, transparent, multifunctional, carbon nanotube sheets. Science 2005;309(5738):1215–9.

[9] Vigolo B, Penicaud A, Coulon C, Sauder C, Pailler R, Journet C, et al. Macroscopic fibers and ribbons of oriented carbon nanotubes. Science 2000;290(5495):1331–4.

[10] Ko F, Gogotsi Y, Ali A, Naguib N, Ye HH, Yang GL, et al. Electrospinning of continuous carbon nanotube-filled nanofiber yarns. Adv Mater 2003;15(14):1161–5.

[11] Zhang XB, Jiang KL, Teng C, Liu P, Zhang L, Kong J, et al. Spinning and processing continuous yarns from 4-inch wafer scale super-aligned carbon nanotube arrays. Adv Mater 2006;18(12):1505–10.

[12] Zhang XF, Li QW, Tu Y, Li YA, Coulter JY, Zheng LX, et al. Strong carbon-nanotube fibers spun from long carbon-nanotube arrays. Small 2007;3(2):244–8.

[13] Tran CD, Humphries W, Smith SM, Huynh C, Lucas S. Improving the tensile strength of carbon nanotube spun yarns using a modified spinning process. Carbon 2009;47(11):2662–70.

[14] Wei Y, Liu L, Liu P, Xiao L, Jiang KL, Fan SS. Scaled fabrication of single-nanotube-tipped ends from carbon nanotube micro-yarns and their field emission applications. Nanotechnology 2008;19(47):475707/1–5.

[15] Aliev AE, Oh JY, Kozlov ME, Kuznetsov AA, Fang SL, Fonseca AF, et al. Giant-stroke, superelastic carbon nanotube aerogel muscles. Science 2009;323(5921):1575–8.

[16] Li QW, Li Y, Zhang XF, Chikkannanavar SB, Zhao YH, Dangelewicz AM, et al. Structure-dependent electrical properties of carbon nanotube fibers. Adv Mater 2007;19(20):3358–63.

[17] Li QW, Zhang XF, DePaula RF, Zheng LX, Zhao YH, Stan L, et al. Sustained growth of ultralong carbon nanotube arrays for fiber spinning. Adv Mater 2006;18(23):3160–5.

[18] Liu K, Sun YH, Chen L, Feng C, Feng XF, Jiang KL, et al. Controlled growth of super-aligned carbon nanotube arrays for spinning continuous unidirectional sheets with tunable physical properties. Nano Lett 2008;8(2):700–5.

[19] Zhang S, Zhu L, Minus ML, Chae HG, Jagannathan S, Wong CP, et al. Solid-state spun fibers and yarns from 1-mm long carbon nanotube forests synthesized by water-assisted chemical vapor deposition. J Mater Sci 2008;43(13):4356–62.

[20] Huynh CP, Hawkins SC. Understanding the synthesis of directly spinnable carbon nanotube forests. Carbon 2010;48(4):1105–15.

[21] Kim JH, Jang HS, Lee KH, Overzet LJ, Lee GS. Tuning of Fe catalysts for growth of spin-capable carbon nanotubes. Carbon 2010;48(2):538–47.

[22] Andrews R, Jacques D, Rao AM, Derbyshire F, Qian D, Fan X, et al. Continuous production of aligned carbon nanotubes: a step closer to commercial realization. Chem Phys Lett 1999;303(5–6):467–74.

[23] Singh C, Shaffer MS, Windle AH. Production of controlled architectures of aligned carbon nanotubes by an injection chemical vapour deposition method. Carbon 2003;41(2):359–68.

[24] Huang JQ, Zhang Q, Wei F, Qian WZ, Wang DZ, Hu L. Liquefied petroleum gas containing sulfur as the carbon source for carbon nanotube forests. Carbon 2008;46(2):291–6.

[25] Kumar M, Okazaki T, Hiramatsu M, Ando Y. The use of camphor-grown carbon nanotube array as an efficient field emitter. Carbon 2007;45(9):1899–904.

[26] Zhang Q, Huang JQ, Zhao MQ, Qian WZ, Wang Y, Wei F. Radial growth of vertically aligned carbon nanotube arrays from ethylene on ceramic spheres. Carbon 2008;46(8):1152–8.

[27] Lv RT, Tsuge S, Gui XC, Takai K, Kang FY, Enoki T, et al. In situ synthesis and magnetic anisotropy of ferromagnetic buckypaper. Carbon 2009;47(4):1141–5.

[28] Zhang Q, Zhou WP, Qian WZ, Xiang R, Huang JQ, Wang DZ, et al. Synchronous growth of vertically aligned carbon nanotubes with pristine stress in the heterogeneous catalysis process. J Phys Chem C 2007;111(40):14638–43.

[29] Huang JQ, Zhang Q, Zhao MQ, Wei F. The release of free standing vertically-aligned carbon nanotube arrays from a substrate using $CO_2$ oxidation. Carbon 2010;48(5):1441–50.

[30] Kunadian I, Andrews R, Qian DL, Menguc MP. Growth kinetics of MWCNTs synthesized by a continuous-feed CVD method. Carbon 2009;47(2):384–95.

[31] Lv RT, Kang FY, Zhu D, Zhu YQ, Gui XC, Wei JQ, et al. Enhanced field emission of open-ended, thin-walled carbon nanotubes filled with ferromagnetic nanowires. Carbon 2009;47(11):2709–15.

[32] Shaffer MSP, Fan X, Windle AH. Dispersion and packing of carbon nanotubes. Carbon 1998;36(11):1603–12.

[33] Wang BN, Bennett RD, Verploegen E, Hart AJ, Cohen RE. Quantitative characterization of the morphology of multiwall carbon nanotube films by small-angle X-ray scattering. J Phys Chem C 2007;111(16):5859–65.

[34] Ding W, Calabri L, Kohlhaas KM, Chen X, Dikin DA, Ruoff RS. Modulus, fracture strength, and brittle vs. plastic response of the outer shell of arc-grown multi-walled carbon nanotubes. Exp Mech 2007;47(1):25–36.

[35] Zhang XH, Li QW. Enhancement of friction between carbon nanotubes: an efficient strategy to strengthen fibers. ACS Nano 2010;4(1):312–6.

[36] Li YL, Kinloch IA, Windle AH. Direct spinning of carbon nanotube fibers from chemical vapor deposition synthesis. Science 2004;304(5668):276–8.

[37] Koziol K, Vilatela J, Moisala A, Motta M, Cunniff P, Sennett M, et al. High-performance carbon nanotube fiber. Science 2007;318(5858):1892–5.

[38] Zhong XH, Li YL, Liu YK, Qiao XH, Feng Y, Liang J, et al. Continuous multilayered carbon nanotube yarns. Adv Mater 2010;22(6):692–6.

[39] Inoue Y, Kakihata K, Hirono Y, Horie T, Ishida A, Mimura H. One-step grown aligned bulk carbon nanotubes by chloride mediated chemical vapor deposition. Appl Phys Lett 2008;92(21):213113/1–3.

[40] Su DS. The use of natural materials in nanocarbon synthesis. ChemSusChem 2009;2(11):1009–20.

[41] Zhang Q, Zhao MQ, Huang JQ, Liu Y, Wang Y, Qian WZ, et al. Vertically aligned carbon nanotube arrays grown on a lamellar catalyst by fluidized bed catalytic chemical vapor deposition. Carbon 2009;47(11):2600–10.

[42] Pint CL, Pheasant ST, Pasquali M, Coulter KE, Schmidt HK, Hauge RH. Synthesis of high aspect-ratio carbon nanotube "flying carpets" from nanostructured flake substrates. Nano Lett 2008;8(7):1879–83.